Bioelectrochemistry 82 (2011) 125–130

Contents lists available at ScienceDirect

Bioelectrochemistry

journal homepage: www.elsevier.com/locate/bioelechem

Direct electrochemistry and electrocatalysis of hemoglobin on chitosan-room temperature ionic liquid-TiO_2-graphene nanocomposite film modified electrode

Jun-Yong Sun, Ke-Jing Huang *, Su-Fang Zhao, Yang Fan, Zhi-Wei Wu

College of Chemistry and Chemical Engineering, Xinyang Normal University, Xinyang 464000, China

ARTICLE INFO

Article history:
Received 24 March 2011
Received in revised form 20 June 2011
Accepted 23 June 2011
Available online 8 July 2011

Keywords:
Hemoglobin
Direct electrochemistry
TiO_2-graphene nanocomposite
Ionic liquid
Hydrogen peroxide

ABSTRACT

TiO_2-graphene nanocomposite was prepared by hydrolysis of titanium isopropoxide in colloidal suspension of graphene oxide and in situ hydrothermal treatment. The direct electrochemistry and electrocatalysis of hemoglobin in room temperature ionic liquid 1-Butyl-3-methylimidazolium hexafluorophosphate, chitosan and TiO_2-graphene nanocomposite modified glassy carbon electrode were investigated. The biosensor was examined by using UV-vis spectroscopy, scanning electron microscopy and electrochemical methods. The results indicated that hemoglobin remained its bioactivity on the modified electrode, showing a couple of well-defined and quasi-reversible redox peaks, corresponding to hemoglobin Fe^{III}/Fe^{II} couple. The kinetic parameters for the electrode reaction, such as the formal potential ($E^{o'}$), the electron transfer rate constant (k_s), the apparent coverage (Γ), and Michaelis–Menten constant (K_m) were evaluated. The biosensor showed good electrochemical responses to the reduction of H_2O_2 in the ranges of 1–1170 μM. The detection limit was 0.3 μM (S/N = 3). The properties of this composite film, together with the bioelectrochemical catalytic activity, could make them useful in the development of bioelectronic devices, and investigation of electrochemistry of other heme proteins at functional interface.

1. Introduction

Recently, development of an electrochemical basis for investigations of protein structure, mechanisms of redox transformation of protein molecules, and metabolic processes involving redox transformations has been paid more and more attention. Understanding of these reactions fundamentally can provide the insight into physiological electron transfer process as well as an impetus to the further development of biosensors and bioelectrocatalytical systems [1–4]. Hemoglobin (Hb) is an important redox respiratory protein in red cells. It contains the porphyrin complex of iron(II) or hemin(III) as a prosthetic group and perform different physiological functions [5,6]. It can be used to catalyze the reduction of hydrogen peroxide (H_2O_2) [7]. Because of its known structure and commercial availability, Hb is considered as an ideal model molecule for heme proteins study [8]. Unfortunately, Hb generally exhibits a rather slow rate of heterogeneous electron transfer and can not exhibit electroactivity at conventional electrodes because of the deep bury of the electroactive prosthetic groups and the unfavorable orientations at electrodes. Therefore, it is a challenge to develop matrix to immobilize Hb. Many materials have been used to immobilize Hb on the surface of electrodes, such as surfactants [9], biopolymers [10], polyelectrolytes [11], nanomaterials like carbon nanotubes [12], quantum dots [13], and mesoporous materials [14].

Among these, room temperature ionic liquids (RTILs) 1-Butyl-3-methylimidazolium hexafluorophosphate ([bmim]PF_6), TiO_2-graphene (TiO_2-Gr) nanocomposite and chitosan (Chit) have become more attractive due to their excellent properties. Ionic liquids (ILs) have attracted much attention as extraordinarily high chemical and thermal stability, good conductivity, wide electrochemical windows, no requirement for additional supporting electrolytes and good dissolving capability. It has been widely used in organic synthesis, liquid–liquid extraction, electrochemistry and inorganic synthesis [15,16]. So far, the application of ILs in electrochemistry has been stretched in many areas, such as the electrodeposition of metals or semiconductors [17], the electropolymerization of organic compounds [18] and the fabrication of gas sensors and supercapacitors [19].

Graphene (Gr) is a flat monolayer of carbon atoms tightly packed into a two-dimensional (2D) honeycomb lattice. Owing to its extraordinary electronic transport properties and high electrocatalytic activities, Gr greatly promotes the electrochemical reactivity of biomolecules on the modified electrode surface [20–22]. Gr-based electrochemical sensors and biosensors have recently received increasing attention in the field of electroanalysis [21–23], such as direct electrochemistry of enzymes [24–26] and small biomolecules detection [27,28]. Due to its good biocompatibility, high conductivity and low cost, TiO_2 in various forms such as nanoparticles, nanoneedles and nanotubes, has become an attractive electrode material for electrochemical sensors and biosensors applications [29–31]. On the other hand, the electrochemical properties of

* Corresponding author. Tel.: +86 376 6390611; fax: +86 376 6390597.
E-mail address: kejinghuang@163.com (K.-J. Huang).

1567-5394/$ – see front matter © 2011 Elsevier B.V. All rights reserved.
doi:10.1016/j.bioelechem.2011.06.007

TiO_2 have shown to be greatly improved in TiO_2-Gr hybrid materials [32,33].

Chitosan (Chit) is a polysaccharide derived by deacetylation of chitin. It possesses many advantages such as excellent membrane-forming ability, high permeability towards water, good adhesion and biocompatibility. Also, it has abundant reactive amino and hydroxyl functional groups [34,35]. So it has been widely used as an immobilization matrix for biofabrication.

Herein, we reported the fabrication, characterization and analytical performance of a biosensor based on Hb/Chit-[bmim]PF_6-TiO_2-Gr nanocomposite modified glassy carbon electrode (GCE). The biosensor showed high sensitivity, improved stability, short response time and wide linear range owing to the synergic effects of Chit, [bmim]PF_6, TiO_2-Gr nanocomposite and Hb molecules. It was successfully used to determine the H_2O_2.

2. Experimental

2.1. Materials

Hb was obtained from Xinjingke Biotechnology Co., Ltd (Beijing, China) and a stock solution of 10 mg mL^{-1} Hb was freshly prepared with a 0.1 M phosphate buffer solutions (PBS, pH 7.0). [bmim]PF_6 was obtained from Chengjie Chemical Co., Ltd (Shanghai, China). Titanium isopropoxide (Ti(O^iPr)$_4$, 98%) was obtained from Aladdin Chemistry Co., Ltd. Chit (92.5% deacetylation) were obtained from Shanghai Reagent Company (Shanghai, China). 0.1 M PBS with various pH values were prepared by mixing stock standard solutions of Na_2HPO_4 and NaH_2PO_4 and adjusted by 0.1 M H_3PO_4 or 0.1 M NaOH solutions. H_2O_2 (30%, w/v) was purchased from Shanghai Chemical Reagent Company (Shanghai, China), its dilute solution was freshly prepared daily and was determined by titration with standard $KMnO_4$ solution. Ultrapure water (18.2 MΩ) was obtained from a Milli-Q water purification system and used throughout. All other chemicals were of analytical grade and used without further purification.

2.2. Instruments

A CHI660D electrochemical workstation (Shanghai ChenHua Instruments Co., China) was used for electrochemical measurements, a standard three-electrode cell contained a platinum wire auxiliary electrode, a saturated calomel reference electrode (SCE) and the modified GCE as working electrode were employed for electrochemical studies. UV-vis spectroscopy was recorded on UVmini-1240 spectrophotometer (Shimadzu Co., Japan). Scanning electron microscopy (SEM) images were obtained on a Hitachi S-4800 scanning electron microscope.

Electrochemical impedance measurements were performed in 0.1 M KCl solution containing 5.0 mM $Fe(CN)_6^{3-}/Fe(CN)_6^{4-}$ (1:1), using an alternating current voltage of 5.0 mV. The frequency range is from 1.0×10^5 Hz to 5×10^{-2} Hz at 25 °C.

During all the experiments, the solutions were thoroughly deoxygenated by bubbling high purity nitrogen for 20 min and a nitrogen atmosphere was maintained over the solutions.

2.3. Preparation of the experimental

A glassy carbon electrode ($d=3$ mm) was polished to a mirror-like surface with 1.0, 0.3 and 0.05 μm aluminum slurry, respectively. Subsequently, the electrode was rinsed with 1:1 HNO_3–H_2O (v/v), ethanol and doubly distilled water in an ultrasonic bath for 2–3 min for each wash and dried under nitrogen at room temperature.

Chit was dissolved in 2.0% (v/v) acetic acid solution and stirred for 2 h to form 0.5% (m/v) solution at room temperature. After undissolved material was filtered, the pH was adjusted using 1.0 M NaOH.

2.4. Fabrication of the electrochemical biosensor

Gr oxide was prepared according to the reported method [36,37]. In short, 20 mg of Gr oxide was dispersed in a mixed solution of H_2O (10 mL) and ethanol (5 mL) under ultrasonication for 1 h to get a homogenous suspension of exfoliated Gr oxide. Then, 0.2 mL of Ti(O^iPr)$_4$ was added to the Gr oxide suspension and ultrasonicated for another 1 h. The resultant mixture was transferred to a 25 mL Teflon-sealed autoclave and kept in oven at 130 °C for 12 h. The final product was isolated by filtration, rinsed thoroughly with deionized water and ethanol, and dried in vacuum. The TiO_2-Gr nanocomposite was obtained in the form of black powder.

The as-prepared TiO_2-Gr and [bmim]PF_6 were dispersed into Chit solution. The mixture was sonicated for 1 h to obtain a homogeneous suspension. The final concentrations of TiO_2-Gr and [bmim]PF_6 were 1 mg mL^{-1} and 2% (v/v) , respectively.

The Chit-[bmim]PF_6-TiO_2-Gr nanocomposite modified GCE was prepared with the following procedure: 10 μL of the resulting mixture was coated at GCE, and then the electrode was dried in the air. Then, a 15 μL of 10 mg mL^{-1} Hb solution (pH 7.0) was cast on the surface of Chit-[bmim]PF_6-TiO_2-Gr nanocomposite modified GCE and dried in the air. The as-prepared Hb/Chit-[bmim]PF_6-TiO_2-Gr/GCE was stored at 4 °C when not in use. For comparison, the Hb/Chit-[bmim]PF_6-Gr/GCE were prepared by the similar way as described above.

The effective surface areas of different modified electrodes were obtained by cyclic voltammetry with 1 mM $K_3Fe(CN)_6$ as a probe at different scan rates. For a reversible process, the following equation applies [38]:

$$i_p = 0.4463\left(F^3/RT\right)^{1/2}An^{3/2}D^{1/2}c\nu^{1/2} \quad (1)$$

where i_p refers to the peak current and A is the electrode area (cm^2). In this work, for 1 mM $K_3Fe(CN)_6$, $T=298$ K (25 °C), $n=1$, $D=7.6\times10^{-6}$ cm^2 s^{-1} (0.1 M KCl), c is the concentration of $K_3Fe(CN)_6$, ν is the scan rate. So, $i_p=2.687\times10^5An^{3/2}D^{1/2}c\nu^{1/2}$, the surface areas of the bare GCE and Chit-[bmim]PF_6-TiO_2-Gr/GCE can be calculated from the slope of the i_p versus $\nu^{1/2}$ plot to be 0.059 cm^2 and 0.187 cm^2, respectively.

3. Results and discussion

3.1. UV-vis spectroscopy

The position of the Soret absorption band of prosthetic heme group can provide information about possible denaturation of hemeproteins, especially that of conformational change in the heme group region [39]. Fig. 1 showed the UV-vis spectra of different films on ITO glass. It was obvious that Hb in Chit-[bmim]PF_6-TiO_2-Gr nanocomposite film (Fig. 1b) and Chit-[bmim]PF_6-Gr film (Fig. 1c) all kept nearly

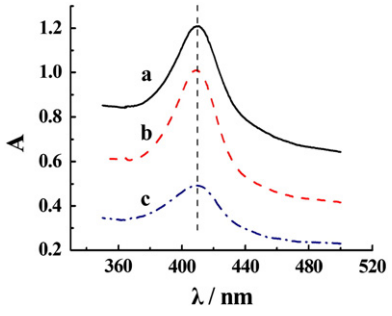

Fig. 1. UV-vis absorption spectra of Hb (a), Hb in Chit-[bmim]PF_6-TiO_2-Gr nanocomposite (b) and Hb/Chit-[bmim]PF_6-Gr (c) films on ITO glass.

the same Soret band as native Hb film (409 nm, Fig. 1a), indicating that Hb in the composite films well maintained its natural state.

3.2. Morphology of Gr and TiO_2-Gr

The morphology of the obtained Gr and TiO_2-Gr were observed by SEM (Fig. 2). In Fig. 2a, it exhibits the SEM image of Gr agglomerate, consisting of almost transparent carbon nanosheets with thin wrinkled structure that Gr owns intrinsically. In Fig. 2b, it can be seen that TiO_2 was formed in a highly faceted morphology on the substrates of Gr.

3.3. Characterization of Hb/Chit-[bmim]PF_6-TiO_2-Gr/GCE

Electrochemical impedance spectroscopy (EIS) was used to monitor the assembly process. Fig. 3 showed the impedance spectra represented as Nyquist plots (*Zim* vs. *Zre*) for bare GCE (a), Chit/GCE (b), Chit-[bmim]PF_6-TiO_2-Gr/GCE (c) and Hb/Chit-[bmim]PF_6-TiO_2-Gr/GCE (d) in 5 mM $Fe(CN)_6^{3-/4-}$ containing 0.1 M KCl solution (pH 7.0), respectively. A straight line was observed at bare GCE (curve a), which implied low resistance. After Chit was coated at GCE (curve b), the diameter of the semicircle increased greatly, showing that the Chit film obstructed the electron transfer of the electrochemical probe. This may be ascribed to the weak conductivity of the Chit film. When Chit-[bmim]PF_6-TiO_2-Gr nanocomposite was assembled at GCE(curve c), it was found that the diameter of the semicircle decreased, suggesting Chit-[bmim]PF_6-TiO_2-Gr nanocomposite was beneficial to the electrons transfer. Moreover, with the assembly of Hb onto the Chit-[bmim]PF_6-TiO_2-Gr/GCE (curve *d*), the semicircular diameter increased again, which was attributed to the further increase of the thickness of the modified film and the non-conductive properties of Hb, suggesting the protein successfully deposited on the outerlayer of Chit-[bmim]PF_6-TiO_2-Gr nanocomposite film modified GCE. The above results could clearly confirm the success of the assembly of the electrode.

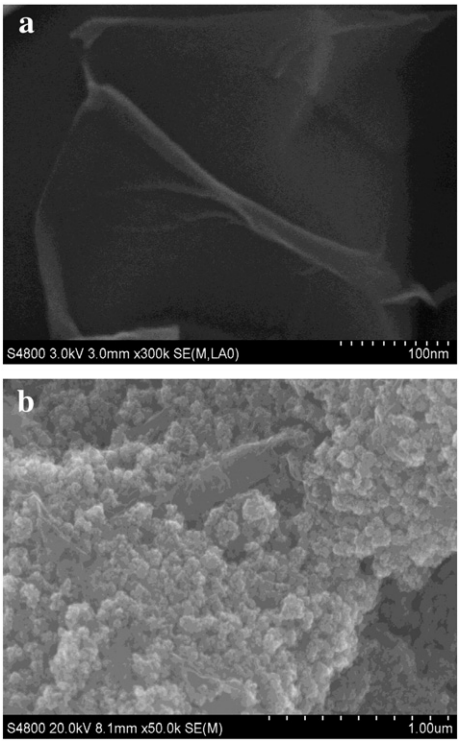

Fig. 2. SEM images of (a) Gr and (b) TiO_2-Gr.

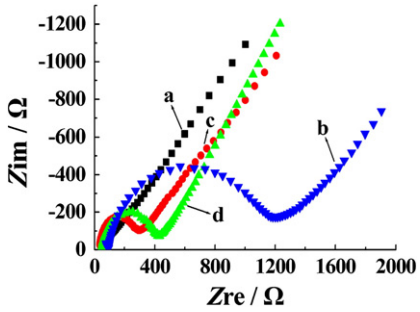

Fig. 3. Nyquist plots of bare GCE (a), Chit/GCE (b), Chit-[bmim]PF_6-TiO_2-Gr/GCE (c) and Hb/Chit-[bmim]PF_6-TiO_2-Gr/GCE (d) in 5 mM $Fe(CN)_6^{3-/4-}$ containing 0.1 M KCl solution (pH 7.0), respectively. The frequency range was from 1.0×10^5 Hz to 5×10^{-2} Hz, and the perturbation signal is 5 mV.

3.4. Electrochemical behaviors of Hb

The electrochemical behavior of different electrodes in 0.1 M PBS (pH 7.0) at 100 mV s^{-1} was studied by cyclic voltammetry. Fig. 4 showed the cyclic voltammograms obtained with bare GCE, Hb/GCE, Chit-[bmim]PF_6-TiO_2-Gr/GCE, Hb/Chit-[bmim]PF_6-Gr/GCE and Hb/Chit-[bmim]PF_6-TiO_2-Gr/GCE, respectively. No redox peaks were observed with bare GCE (curve a), Hb/GCE (curve b) and Chit-[bmim]PF_6-TiO_2-Gr/GCE (curve c), However, a couple of redox peaks were observed at Hb/Chit-[bmim]PF_6-Gr/GCE (curve d). The reason may be that Chit-[bmim]PF_6-Gr film provided a good microenvironments and more effective adsorption of Hb. The good conductive ability of the composite film improves the electron transfer between the protein and the electrode.

Compared with curve d, a couple of well-defined and nearly symmetrical redox peaks were observed with Hb/Chit-[bmim]PF_6-TiO_2-Gr/GCE (curve e), and the peak currents were much larger with the Hb/Chit-[bmim]PF_6-Gr/GCE. The anodic peak potential (E_{pa}) and the cathodic peak potential (E_{pc}) were located at about −0.148 and −0.265 V, respectively. The formal potential ($E^{o'}$), defined as the average of E_{pa} and E_{pc}, was about −0.206 V. This illuminated that the redox peaks in curve e attribute to the electrochemical reaction of the Fe(III)/Fe(II) couple of Hb. The improved electrochemical responses could be attributed to the direct electron transfer of Hb with the help of Chit-[bmim]PF_6-TiO_2-Gr nanocomposite film. In the composite film, the [bmim]PF_6 has a good conductivity and Chit possess good membrane-forming ability and biocompatibility. TiO_2-Gr has good conductive ability and electrocatalysis. The synergic effects of [bmim]PF_6, Chit and TiO_2-Gr greatly improved the electrochemical performance of the modified electrode.

The redox currents of the Hb/Chit-[bmim]PF_6-TiO_2-Gr/GCE were dependent on the scan rates. Fig. 5 showed the cyclic voltammograms of the Hb/Chit-[bmim]PF_6-TiO_2-Gr/GCE in 0.1 M PBS (pH 7.0) at various scan rates. It could be seen that the redox peak currents

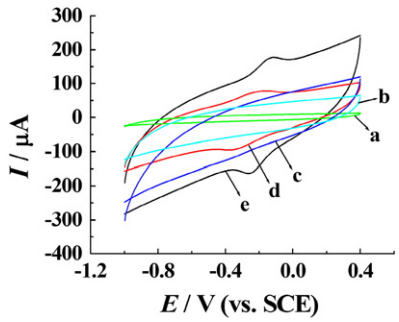

Fig. 4. Cyclic voltammograms of bare GCE (a), Hb/GCE (b), Chit-[bmim]PF_6-TiO_2-Gr/GCE (c), Hb/Chit-[bmim]PF_6-Gr/GCE (d) and Hb/Chit-[bmim]PF_6-TiO_2-Gr/GCE (e) in 0.1 M PBS (pH 7.0) with a scan rate of 100 mV s^{-1}.

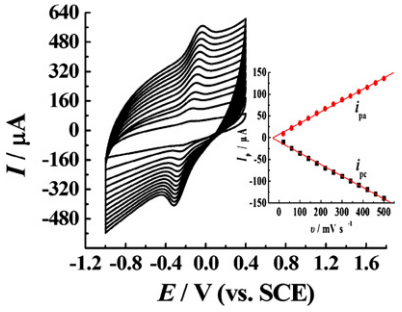

Fig. 5. Cyclic voltammograms of Hb/Chit-[bmim]PF_6-TiO_2-Gr/GCE in 0.1 M PBS (pH 7.0) at different scan rates (from inner to outer) of 20, 60, 100, 140, 180, 220, 260, 300, 340, 380, 420, 460 and 500 mV s^{-1} (inset: the relationship between the peak currents i_p vs. the sweep rates υ).

increase and the redox peak potentials shift simultaneously with the increase of scan rates, and the peak-to-peak separation become greater, indicating the more irreversible of the electrode process. The redox peak currents had almost the same values in the selected range of scan rates, and the oxidation and reduction peak heights were nearly equal to each other within all scans rate ranges (the ratio of oxidation and reduction peak currents was about 1.112). This indicated that nearly all the electroactive ferrous species (Hb-Fe (II)), which was produced by reduction of ferric species (Hb-Fe(III)) during the potential scan of +0.4 to −1.0 V, were oxidized to Hb-Fe (III) on the reverse scan. The anodic and cathodic peak currents were proportional to scan rates from 20 to 500 mV s^{-1} (see the inset in Fig. 5). Linear regression equations were obtained as $i_{pa}/\mu A = 7.256 + 0.261\ \upsilon/\text{mV s}^{-1}$ ($R = 0.999$, $n = 13$), and $i_{pc}/\mu A = -8.879 - 0.264\ \upsilon/\text{mV s}^{-1}$ ($R = 0.998$, $n = 13$), suggesting that the reaction was characteristic of surface or thin layer electrochemistry.

According to Faraday's law

$$Q = nFA\Gamma \tag{2}$$

Laviron's equation [40]

$$I_p = n^2F^2Av\Gamma / 4RT \tag{3}$$

can be changed as $I_p = nFQ\upsilon/4RT$, where Γ is the surface coverage of the electrode reaction substance (mol cm^{-2}), A is the electrode area (cm^2), and Q is the quantity of charge (C), calculated from the reduction peak area of the voltammogram, and n, I_p, F, R, and T have their usual meanings. From the slope of the I_{pc} versus υ plot, n was calculated to be 1.03, and 1.08 from the I_{pa} versus υ plot, indicating a one-electron redox reaction of Hb/Chit-[bmim]PF_6-TiO_2-Gr/GCE [41,42].

The charges and thus the average surface concentration of electroactive species can be calculated from the following equation: $Q = nFA\Gamma$. Thus, the average surface concentration of electroactive Hb (Γ) in Chit-[bmim]PF_6-TiO_2-Gr/GCE surface was estimated to be 3.21×10^{-10} mol cm^{-2}. A 15 μL aliquot of the Hb solution (pH 7.0) was cast onto the Chit-[bmim]PF_6-TiO_2-Gr/GCE surface, the total amount of deposited Hb is 2.33×10^{-9} mol. For Hb, the electroactive amount obtained here accounts for about 13.7%. The fact that the fraction of electroactive Hb obtained here is higher than those of immobilizing Hb in protein-gluten films (4.9%) [43] or dimyristoyl phosphatidylcholine films (8%) [44]. The electron transfer rate (k_s) of Hb in Chit-[bmim]PF_6-TiO_2-Gr nanocomposite film was evaluated based on the model of Laviron [40] with the formula $k_s = mnF\upsilon/RT$, where m is a parameter related to the peak-to-peak separation, the value of k_s varies from 0.73 to 3.96 s^{-1} was obtained at a scan rate of 20–500 mV s^{-1}.

3.5. Effect of pH

The pH is essential to the electrochemical behaviors of proteins. Because it was proton participated in the redox process, the immobilized Hb also showed strong dependence on solution pH (data not shown). In the pH range of 3.0–10.0, the peak potentials shifted negatively and the maximum peak currents obtained at pH 7.0. Therefore, pH 7.0 PBS was chosen as buffer solution in the following experiment. All changes in cyclic voltammograms peak potentials and currents with pH were reversible. Moreover, the effect of solution pH on $E^{o'}$ of Hb showed linear response with a slope about −39 mV pH^{-1}, much smaller than that of theoretical value [45] of −58 mV pH^{-1} for a reversible single electron transfer coupled with proton, but similar to those observed at {Hb/CMK-3}$_6$ film electrode [46] and Hb-mesoporous WO_3 film electrode [47,48], the electrochemical reaction can be expressed as follows:

$$\text{HbFe(III)} + H^+ + e^- \rightleftharpoons \text{HbHFe(II)} \tag{4}$$

The reason might be the influence of the protonation states of trans ligands to the heme iron and amino acids around the heme, or the protonation of the water molecule coordinated to the central iron [45].

3.6. Electrocatalytic response of H_2O_2 at Hb/Chit-[bmim]PF_6-TiO_2-Gr/GCE

The amperometric response to H_2O_2 at the Hb/Chit-[bmim]PF_6-TiO_2-Gr/GCE was investigated by successively adding H_2O_2 to a continuous stirring PBS solution under the optimized conditions. Fig. 6 showed the steady-state amperometric response of the biosensor to the successive addition of aliquot H_2O_2 into the PBS (pH 7.0) with an operating potential of −300 mV. When 30 μM H_2O_2 was added, the background current was changed and the reduction current rose steeply to reach the maximum value. This sensor could achieve more than 95% of the steady-state current within 2.5 s, indicating a fast amperometric response to H_2O_2 reduction. Also, the increasing H_2O_2 concentration resulted in an increase of the amperometric response. Under the optimized experimental parameters, the sensor showed a linear response within the range of 1.0×10^{-6} to 1.17×10^{-3} M of H_2O_2. The calibration plot over

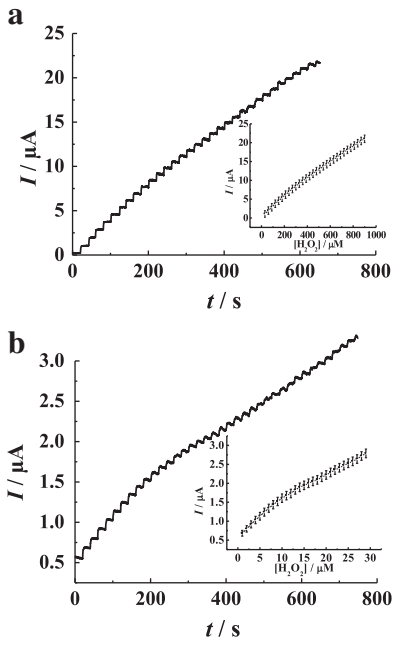

Fig. 6. Amperometric response of Hb/Chit-[bmim]PF_6-TiO_2-Gr/GCE to H_2O_2, (a) successive addition of 30 μM and (b) 1 μM. Conditions −300 mV constant potential, pH 7.0 and rotation speed is 2000 rpm.

the concentration range 1–30 μM (30 points) is expressed by a linear regression equations as $I/\mu A = 0.8033 + 0.0707\ c(H_2O_2)/\mu M$, and had a slope of 0.0707 μA μM^{-1} with a correlation coefficient of 0.994. The detection limit was determined to be 3.0×10^{-7} M (S/N = 3). The performance of the developed biosensor was compared with other electrochemical methods, and the results were shown in Table 1. The developed method in this work showed high sensitivity and wide linear range, and was suitable to be the most commonly used analytical method for detecting low concentration of H_2O_2.

The apparent Michaelis–Menten constant K_m, which gives an indication of the enzyme-substrate kinetics, can be obtained from the Lineweaver–Burk equation [49]: $1/I_{ss} = 1/I_{max} + K_m/I_{max}.1/c$, where c is the concentration of H_2O_2 in solution, I_{ss} is the catalytic reduction current (background current deducted) at the steady state when H_2O_2 concentration is at c, and I_{max} is the maximum catalytic current. K_m can be obtained by the analysis of the slope and the intercept of the plot of the reciprocals of the steady-state current versus H_2O_2 concentration. In this work, the linear equation was expressed as: $1/(I_{ss}/\mu A) = 0.02259 + 28.1335\ 1/[c(H_2O_2)/\mu M]$ ($R = 0.9994$), and the K_m value for the electrocatalytic activity of Hb/Chit-[bmim]PF_6-TiO_2-Gr/GCE to H_2O_2 was determined to be 1.245 mM, which implied that the present electrode exhibited a higher affinity for H_2O_2. As was well known the smaller K_m showed the higher catalytic ability. The low value of K_m indicated that Hb immobilized in Chit-[bmim]PF_6-TiO_2-Gr nanocomposite film retained its bioactivity and had a high biological affinity to H_2O_2.

3.7. Stability and repeatability of Hb/Chit-[bmim]PF_6-TiO_2-Gr/GCE

The modified electrode showed an acceptable stability and repeatability. When not in use, the modified electrode was stored in pH 7.0 PBS at 4 °C for about 20 days, it retained about 95% of its initial current responds, and the relative standard deviation (R.S.D) was 4.4% for nine successive determinations of a 5.0×10^{-5} M H_2O_2 with the modified electrode. When the modified electrode was successively scanned for 100 cycles, no obvious change in the peak current could be observed (<3.0%). The fabrication of seven modified electrodes made independently, showed a good reproducibility with R.S.D. 5.36% for the current determined in the presence of 5.0×10^{-5} M H_2O_2.

3.8. Selectivity of the H_2O_2 biosensor

Selectivity is important in practical use of the biosensors, and the selectivity of the Hb/Chit-[bmim]PF_6-TiO_2-Gr/GCE biosensor was evaluated with six interfering substances (acetic acid, glucose, ethanol, ascorbic acid, uric acid and L-tyrosine) by using cyclic voltammetry. The current ratios were calculated by reading the current of the developed biosensor in the solution containing 1.0×10^{-4} M H_2O_2 and 2.0×10^{-4} M interfering substance and comparing it with the current from the biosensor in the solution containing only 1.0×10^{-4} M H_2O_2. Tests showed that the six tested substances did not interfere significantly with the resulting biosensor (signal change below 5%).

Table 1
The performances of the various types of modified electrodes.

Modified electrodes	Linear range/(μM)	LOD/(μM)	Stability[a]/(percentage/days)	Reference
Hb in nano-Au/ITO	10–7000	4.5	75%/40	[50]
Hb in egg phosphatidylcholine/pyrolytic graphite electrode	10–100	3.90	90%/14	[51]
Hb in silica sol–gel/ carbon paste electrode	1–280	0.86	93%/21	[52]
Hb in carbon nanotube powder microelectrodes electrodes	210–900	9.00	Not reported	[53]
Hb in thiolated-viologen/Au electrode	10–125	0.25	90%/30	[54]
Hb in CHT/nano-$CaCO_3$/GCE	37–830	8.30	Not reported	[55]
Hb in Chit-[bmim]PF_6-TiO_2-Gr/GCE	1–1170	0.3	95%/20	This work

[a] The biosensor retained percentage of its initial response after a storage period.

3.9. Recovery experiment

The analytical applicability of the developed biosensor was evaluated by determining the recoveries of 0.2, 0.4, 0.6 and 0.8 mM H_2O_2 by standard addition method. The recovery rate of the developed biosensor was 99.1% (0.196 ± 0.008 mM, $n = 3$, R.S.D. = 4.3%), 97.2% (0.392 ± 0.018 mM, $n = 3$, R.S.D. = 4.1%), 98.8% (0.591 ± 0.035 mM, $n = 3$, R.S.D. = 4.6%) and 98.6% (0.79 ± 0.047 mM, $n = 3$, R.S.D. = 4.7%), respectively.

4. Conclusions

In this work, we have demonstrated a simple method for designing a H_2O_2 biosensor using Hb immobilized in a Chit-[bmim]PF_6-TiO_2-Gr nanocomposite modified GCE. Chit-[bmim]PF_6-TiO_2-Gr nanocomposite film showed a suitable biocompatible microenvironment for Hb. The catalytic properties proved that the Hb has been kept in its natural structure and can retain its biological activity. The modified electrode had good stability and reproducibility, high sensitive and selective, and showed good electrocatalytic responses to the reduction of H_2O_2 in the ranges of 1–1170 μM. The detection limit was 0.3 μM (S/N = 3). The properties of this composite film, together with the bioelectrochemical catalytic activity, could make them useful in the development of bioelectronic devices, and investigation electrochemistry of other heme proteins at functional interface.

Acknowledgments

This work was supported by the National Natural Science Foundation of China (20805040), Program for Science & Technology Innovation Talents in Universities of Henan Province (2010HASTIT025), and Excellent Youth Foundation of He'nan Scientific Committee (104100510020).

References

[1] Q.I. Wang, G.X. Lu, B.J. Yang, Myoglobin/sol–gel film modified electrode: direct electrochemistry and electrochemical catalysis, Langmuir 20 (2004) 1342–1347.
[2] J.X. Li, L.H. Zhou, H. Xia, J. Hu, H.L. Liu, J. Xu, Direct electrochemistry of hemoglobin immobilized on siliceous mesostructured cellular foam, Sens Actuators: B. 138 (2009) 545–549.
[3] K. Zhang, L.Y. Mao, R.X. Cai, Stopped-flow spectrophotometric determination of hydrogen peroxide with hemoglobin as catalyst, Talanta 51 (2000) 179–186.
[4] F.G. Parak, G.U. Nienhaus, Myoglobin, a paradigm in the study of protein dynamics, Chemphyschem 3 (2002) 249–254.
[5] F.A. Armstrong, G.S. Wilson, Recent developments in faradaic bioelectrochemistry, Electrochim. Acta. 45 (2000) 2623–2645.
[6] I. Hamachi, A. Fujita, T. Kunitake, Protein engineering using molecular assembly: functional conversion of cytochrome *c* via noncovalent interactions, J. Am. Chem. Soc. 119 (1997) 9096–9102.
[7] A. Jitianu, T. Cacciaguerra, M.H. Berger, R. Benoit, F. B´eguin, S. Bonnamy, New carbon multiwall nanotubes–TiO_2 nanocomposites obtained by the sol–gel method, J. Non-Cryst. Solids. 345–346 (2004) 596–600.
[8] Z. Li, N. Hu, Direct electrochemistry of heme proteins in their layer-by-layer films with clay nanoparticles, J. Electroanal. Chem. 558 (2003) 155–165.
[9] X.Y. He, L. Zhu, Direct electrochemistry of hemoglobin in cetylpyridinium bromide film: redox thermodynamics and electrocatalysis to nitric oxide, Electrochem. Commun. 8 (2006) 615–620.
[10] Q. Lu, T. Zhou, S.S. Hu, Direct electrochemistry of hemoglobin in PHEA and its catalysis to H_2O_2, Biosens. Bioelectron. 22 (2007) 899–904.
[11] H. Sun, N.F. Hu, Size effect of polystyrene (PS) latex beads on electrochemical and electrocatalytic activity of layer-by-layer films of heme protein-coated PS beads with polyelectrolytes, J. Electroanal. Chem. 588 (2006) 207–217.

[12] L.Y. Zhao, H.Y. Liu, N.F. Hu, Assembly of layer-by-layer films of heme proteins and single-walled carbon nanotubes: electrochemistry and elelctrocatalysis, Anal. Bioanal. Chem. 384 (2006) 414–422.
[13] Q. Lu, S.S. Hu, D.W. Pang, Z.K. He, Direct electrochemistry and electrocatalysis with hemoglobin in water-soluble quantum dots film on glassy carbon electrode, Chem. Commun. 20 (2005) 2584–2585.
[14] Y.Z. Xian, Y. Xian, L.H. Zhou, F.H. Wu, Y. Ling, L.T. Jin, Encapsulation hemoglobin in ordered mesoporous silicas: influence factors for immobilization and bioelectrochemistry, Electrochem. Commun. 9 (2007) 142–148.
[15] J. Dupont, R.F. de Souza, P.A.Z. Suarez, Ionic liquid (molten salt) phase organometallic catalysis, Chem. Rev. 102 (2002) 3667–3692.
[16] Y. Zhou, J.H. Schattka, M. Antonietti, Room-temperature ionic liquids as template to monolithic mesoporous silica with wormlike pores via a sol–gel nanocasting technique, Nano. Lett. 4 (2004) 477–481.
[17] Z. Li, H. Liu, Y. Liu, P. He, J. Li, A room-temperature ionic-liquid-templated proton-conducting gelatinous electrolyte, J. Phys. Chem. B. 108 (2004) 17512–17518.
[18] C.L. Aravinda, W. Freyland, Electrodeposition of monodispersed Fe nanocrystals from an ionic liquid, Chem. Commun. 23 (2004) 2754–2755.
[19] S. Zein El Abedin, N. Borissenko, F. Endres, Electropolymerization of benzene in a room temperature ionic liquid, Electrochem. Commun. 6 (2004) 422–426.
[20] D. Li, R.B. Kaner, Graphene-based materials, Science 320 (2008) 1170–1171.
[21] Y.Y. Shao, J. Wang, H. Wu, J. Liu, I.A. Aksay, Y.H. Lin, Graphene based electrochemical sensors and biosensors: a review, Electroanalysis 22 (2010) 1027–1036.
[22] M. Pumera, A. Ambrosi, A. Bonanni, E.L.K. Chng, H.L. Poh, Graphene for electrochemical sensing and biosensing, Trends Anal. Chem. 29 (2010) 954–965.
[23] D. Chen, L. Tang, J. Li, Graphene-based materials in electrochemistry, Chem. Soc. Rev. 39 (2010) 3157–3180.
[24] X. Kang, J. Wang, H. Wu, I.A. Aksay, J. Liu, Y. Lin, Glucose oxidase–graphene–chitosan modified electrode for direct electrochemistry and glucose sensing, Biosens. Bioelectron. 25 (2009) 901–905.
[25] J.F. Wu, M.Q. Xu, G.C. Zhao, Graphene-based modified electrode for the direct electron transfer of cytochrome *c* and biosensing, Electrochem. Commun. 12 (2010) 175–177.
[26] K. Liu, J. Zhang, G. Yang, C. Wang, J.J. Zhu, Direct electrochemistry and electrocatalysis of hemoglobin based on poly(diallyldimethylammonium chloride) functionalized graphene sheets/room temperature ionic liquid composite film, Electrochem. Commun. 12 (2010) 402–405.
[27] M. Zhou, Y.M. Zhai, S.J. Dong, Electrochemical sensing and biosensing platform based on chemically reduced graphene oxide, Anal. Chem. 81 (2009) 5603–5613.
[28] Y. Wang, Y.M. Li, L.H. Tang, J. Lu, J.H. Li, Application of graphene-modified electrode for selective detection of dopamine, Electrochem. Commun. 11 (2009) 889–892.
[29] Y.P. Luo, H.Q. Liu, Q. Rui, Y. Tian, Detection of extracellular H_2O_2 released from human liver cancer cells based on TiO_2 nanoneedles with enhanced electron transfer of cytochrome *c*, Anal. Chem. 81 (2009) 3035–3041.
[30] H. Tang, F. Yan, Q.D. Tai, H.L.W. Chan, The improvement of glucose bioelectrocatalytic properties of platinum electrodes modified with electrospun TiO_2 nanofibers, Biosens. Bioelectron. 25 (2010) 1646–1651.
[31] S.J. Bao, C.M. Li, J.F. Zang, X.Q. Cui, Y. Qiao, J. Guo, New nanostructured TiO_2 for direct electrochemistry and glucose sensor applications, Adv. Funct. Mater. 18 (2008) 591–599.
[32] D. Wang, D. Choi, J. Li, Z. Yang, Z. Nie, R. Kou, D. Hu, C. Wang, L.V. Saraf, J. Zhang, I.A. Aksay, J. Liu, Self-assembled TiO_2–graphene hybrid nanostructures for enhanced li-ion insertion, ACS Nano. 4 (2009) 907–914.
[33] Y.B. Tang, C.S. Lee, J. Xu, Z.T. Liu, Z.H. Chen, Z. He, Y.L. Cao, G. Yuan, H. Song, L. Chen, L. Luo, H.M. Cheng, W.J. Zhang, I. Bello, S.T. Lee, Incorporation of graphenes in nanostructured TiO_2 films via molecular grafting for dye-sensitized solar cell application, ACS Nano. 4 (2010) 3482–3488.
[34] M. Zhang, W. Gorski, Electrochemical sensing platform based on the carbon nanotubes/redox mediators-biopolymer system, J. Am. Chem. Soc. 127 (2005) 2058–2059.
[35] Y. Liu, M.K. Wang, F. Zhao, Z.A. Xu, S.J. Dong, The direct electron transfer of glucose oxidase and glucose biosensor based on carbon nanotubes/chitosan matrix, Biosens. Bioelectron. 21 (2005) 984–988.
[36] W. Hummers, R. Offeman, Graphite oxide was prepared from SP1 graphite, J. Am. Chem. Soc. 80 (1958) 1339.
[37] N.I. Kovtyukhova, P.J. Ollivier, B.R. Martin, T.E. Mallouk, S.A. Chizhik, E.V. Buzaneva, A.D. Gorchinskiy, Layer-by-layer assembly of ultrathin composite films from micron-sized graphite oxide sheets and polycations, Chem. Mater. 11 (1999) 771–778.
[38] A.J. Bard, L.R. Fanlkner, Electrochemical Methods Fundamentals and Applications, Wiley, New York, 1980 p. 258–265.
[39] G. Irace, E. Bismuto, F. Savy, G. Colonna, Unfolding pathway of myoglobin: molecular properties of intermediate forms, Arch. Biochem. Biophys. 244 (1986) 459–469.
[40] E. Laviron, General expression of the linear potential sweep voltammogram in the case of diffusionless electrochemical systems, J. Electroanal. Chem. 101 (1979) 19–28.
[41] G.Y. Shi, Z.Y. Sun, M.C. Liu, L. Zhang, Y. Liu, Y.H. Qu, L.T. Jin, Electrochemistry and electrocatalytic properties of hemoglobin in layer-by-layer films of SiO_2 with Vapor-surface sol–gel deposition, Anal. Chem. 79 (2007) 3581–3588.
[42] W. Sun, R.F. Gao, K. Jiao, Electrochemistry and electrocatalysis of hemoglobin in nafion/nano-$CaCO_3$ film on a new ionic liquid $BPPF_6$ modified carbon paste electrode, J. Phys. Chem. B. 111 (2007) 4560–4567.
[43] H.Y. Liu, N.F. Hu, Heme protein–gluten films: voltammetric studies and their electrocatalytic properties, Anal. Chim. Acta 481 (2003) 91–99.
[44] J. Yang, N. Hu, Direct electron transfer for hemoglobin in biomembrane-like dimyristoyl phosphatidylcholine films on pyrolytic graphite electrodes, Bioelectrochem. Bioenerg. 48 (1999) 117–127.
[45] I. Yamazaki, T. Araiso, Y. Hayashi, H. Yamada, R. Makino, Analysis of acid–base properties of peroxidase and myoglobin, Adv. Biophys. 11 (1978) 249–281.
[46] J.J. Feng, J.J. Xu, H.Y. Chen, Direct electron transfer and electrocatalysis of hemoglobin adsorbed on mesoporous carbon through layer-by-layer assembly, Biosens. Bioelectron. 22 (2007) 1618–1624.
[47] J.J. Feng, J.J. Xu, H.Y. Chen, Direct electron transfer and electrocatalysis of hemoglobin adsorbed onto electrodeposited mesoporous tungsten oxide, Electrochem. Commun. 8 (2006) 77–82.
[48] Q.W. Li, G.A. Luo, J. Feng, Direct electron transfer for heme proteins assembled on nanocrystalline TiO_2 Film, Electroanalysis 13 (2001) 359–363.
[49] J. Li, S.N. Tan, H. Ge, Silica sol-gel immobilized amperometric biosensor for hydrogen peroxide, Anal. Chim. Acta 335 (1996) 137–145.
[50] J.D. Zhang, M. Oyama, A hydrogen peroxide sensor based on the peroxidase activity of hemoglobin immobilized on gold nanoparticles-modified ITO electrode, Electrochim. Acta. 50 (2004) 85–90.
[51] X.J. Han, W.M. Huang, J.B. Jia, S.J. Dong, E.K. Wang, Direct electrochemistry of hemoglobin in egg–phosphatidylcholine films and its catalysis to H_2O_2, Biosens. Bioelectron. 17 (2002) 741–746.
[52] L. Wang, G.X. Lu, B.J. Yang, Hydrogen peroxide biosensor based on direct electrochemistry of hemoglobin immobilized on carbon paste electrode by a silica sol–gel film, Sens, Actuators, B, Chem. 99 (2004) 50–57.
[53] Y.D. Zhao, Y.H. Bi, W.D. Zhang, Q.M. Luo, The interface behavior of hemoglobin at carbon nanotube and the detection for H_2O_2, Talanta 65 (2005) 489–494.
[54] A.K.M. Kafi, D.Y. Lee, S.H. Park, Y.S. Kwon, Development of peroxide biosensor of thiolated-viologen and hemoglobin-modified gold electrode, Microchem. J. 85 (2007) 308–313.
[55] D. Shan, S.X. Wang, H.G. Xue, S. Cosnier, Direct electrochemistry and electrocatalysis of hemoglobin entrapped in composite matrix based on chitosan and $CaCO_3$ nanoparticles, Electrochem. Commun. 9 (2007) 529–534.